Ionic conductivity of ZrO_2-12 mol % Y_2O_3 single crystals

J. D. Solier and I. Cachadiña

Departamento de Física, Universidad de Extremadura, 06071 Badajoz, Spain

A. Dominguez-Rodriguez

Departamento Física Materia Condensada, Facultad de Física, Universidad de Sevilla, Sevilla, Spain

Fast ionic conductors are important to study because of their use in the construction of technological-ly useful devices such as electrochemical cells, oxygen monitors, and the high-temperature fuel cell. Oxygen-ion conductors form a major subgroup of these materials, and, in particular, stabilized zirconia is one of the more important solid electrolytes. However, the ionic conductivity of this material is still only rather poorly understood. The aim of the present work is to describe, by means of a method of lo-cal fits (LF's) to Arrhenius's law, the experimental values of the ionic conductivity of ZrO_2-12 mol % Y_2O_3 single crystals in the temperature range from 200 °C to 1600 °C. This method yields two sets of data: the preexponential factor, A_{LF_i}, and the activation enthalpy, ΔH_{LF_i}. The $\ln A_{LF_i}$ versus $\Delta S(T)/k$ plot [where $\Delta S(T)$ is the entropy change in the process] is a very good test of the accuracy of the LF method. The ΔH_{LF_i} values are fitted by a least-squares procedure to an empirical temperature-dependence function with four adjustable parameters. In order to interpret these results and to under-stand the physical meaning of the fitted parameters, a microscopic model is proposed that allows us to deduce a theoretical function of temperature for the activation enthalpy similar to the empirical func-tion. Then, from this function, we determine the association (0.57 eV) and migration (0.73 eV) enthalpies for oxygen vacancies, and analyze the temperature variation of the free energy (ΔG) and entropy (ΔS), as well as the degree of dissociation of the vacancies in the conduction process for this material. A noteworthy result is that, for the range of temperature studied here, the extrinsic dissociated regime (where it is assumed that all oxygen vacancies are free) is never reached. Finally, taking into account the contribution of the jumps up to the second-next-nearest anionic neighbors, we obtain the value of 1.31×10^{13} Hz for the attempt frequency of the oxygen vacancies.

I. INTRODUCTION

Cubic Y_2O_3-stabilized ZrO_2 is among the more impor-tant solid electrolytes. Nevertheless, its conductivity temperature behavior is still not understood. We think that the main reason for this is that the normal method used to fit experimental data is inadequate. If the ionic conductivity of these materials is represented by a con-ventional Arrhenius plot ($\ln \sigma T$ versus $1/T$), a small and gradual decrease in the slope is observed when the tem-perature is raised.[1-10] This effect is more pronounced in cubic samples with the lowest concentration of yttria.[9,10] The slope of a conventional Arrhenius plot yields the process enthalpy (or activation enthalpy), which contains the true activation enthalpy for defect formation. How-ever, for an oxide ionic conductor in the extrinsic regime, the carrier concentration may be regarded as independent of temperature.[11] In these materials the experimental data are usually fitted by two straight lines. One is for low temperatures (< 700 °C), designated the extrinsic as-sociated regime, in which it is assumed that all oxygen vacancies are associated, forming clusters, and where the activation enthalpy (ΔH) can be written as[12]

$$\Delta H = E_a + E_m , \qquad (1)$$

where E_a and E_m are, respectively, the association and

migration energies for vacancies. The other is for high temperatures (> 900 °C), the extrinsic dissociated regime, in which it is assumed that all oxygen vacancies are free, so that the activation enthalpy is[12]

$$\Delta H = E_m . \qquad (2)$$

This behavior can be correlated with the idea that there are two kinds of oxygen vacancies in the material: those that are single and those forming clusters. At low temperatures the change in the slope is so small that the experimental results can be fitted by a single straight line. However, at high temperatures the gradual decrease in the slope is significant up to 1600 °C, so that a single straight line is not a good fit to the experimental results. To study the conductivity-temperature behavior in these materials, it is therefore necessary to fit all the experi-mental temperature range with a single function.

Recently, Bates and Wang[13] and Suzuki and Sugiya-ma[14] assumed a particular function of the temperature for the activation enthalpy to fit their experimental re-sults. Bates and Wang, in the temperature range from 25 to 450°C, found an activation enthalpy in agreement with the one reported in the literature.[1-10] This concordance is because in this temperature range there is only a very small deviation from linear behavior. By contrast, the ac-tivation enthalpy found by Suzuki and Sugiyama in the

temperature range 700–1600 °C is smaller than the one in the literature.[4,9] This discrepancy is because they interpret the activation enthalpy as a parameter which is a function of T obtained by an Arrhenius fit of the experimental results, but use a temperature-independent preexponential term.[14–16]

In the present work, the experimental value of the ionic conductivity of ZrO$_2$–12 mol % Y$_2$O$_3$ single crystals, in the temperature range 200–1600 °C, was fitted by a local-fit (LF) method to Arrhenius's law.[15] At the same time, the activation enthalpies for association and migration of the oxygen vacancies were determined, as well as the variation with temperature of the free energy (ΔG), entropy (ΔS), and activation enthalpy (ΔH) of the ionic conductivity process in this material.

II. EXPERIMENTAL PROCEDURE

The dc ionic conductivity of single-crystal 12 mol % Y$_2$O$_3$ fully stabilized ZrO$_2$ is studied in the present work. The data were obtained using the four-probe method, from 200 to 850 °C, being results from our laboratory, and from 700 to 1600 °C taken from the work of Suzuki and Sugiyama.[14]

The samples were oriented by the Laue x-ray backreflection technique and cut with a diamond saw into a parallelepiped shape (7.9×3.6×3 mm^3), all the faces being parallel to {100}. The faces were polished and then finished with 3-μm diamond paste. Four 0.3-mm-deep notches separated about 1 mm were cut into lateral faces to facilitate electrical contact, and gold-wire probes were attached with gold paste. Subsequently, the samples were heated to 800 °C to burn off organic residues.

The direct-current electrical conductivity was measured, by the four-probe method, using an electrometer (Keithley model 617) and a current source (1 pA–100 mA, Keithley model 220), both programmable. The two extreme probes were connected to a constant-current source and the potential difference between the two central probes was determined. For a given temperature, the current was adjusted to give a 1-V potential drop between the central probes. The temperature was controlled to within ±1 °C in all cases.

III. LOCAL FIT OF ARRHENIUS'S LAW

The usual way to write the ionic conductivity for a doped oxide conductor is

$$\sigma T = A \exp(-\Delta H /kT) , \qquad (3)$$

where σ is the ionic conductivity, T the absolute temperature, k the Boltzmann constant, A a preexponential term, and ΔH the process-activation enthalpy, A and ΔH being independent of T. If we plot $\ln(\sigma T)$ versus $1/T$, we obtain a straight line with slope $\Delta H /k$ (linear Arrhenius behavior). However, there are ceramic materials for which this behavior is nonlinear. If we plot $\ln(\sigma T)$ versus $1/T$ in the temperature range from 200 to 1600 °C for single-crystal 12 mol % Y$_2$O$_3$–ZrO$_2$ (see Fig. 1), a small and gradual decrease in the slope is observed as the temperature rises. The slope in this plot is temperature
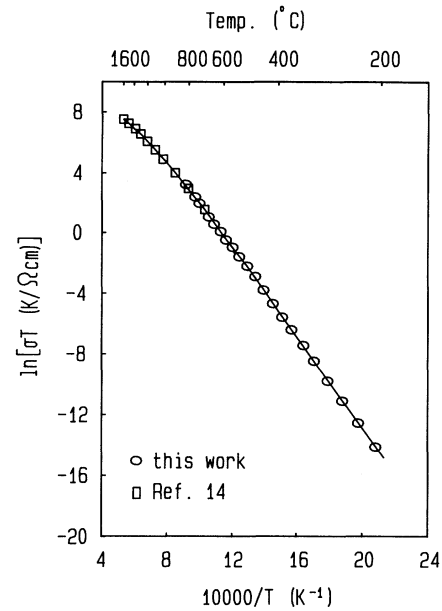

FIG. 1. Arrhenius plot of electrical conductivity of ZrO$_2$–12 mol % Y$_2$O$_3$, with our data and data of Suzuki and Sugiyama (Ref. 14).

dependent, and the physical meaning is not clear.[16]

The LF of the experimental data to an Arrhenius expression allows us to analyze the conductivity over the whole temperature range, maintaining a physical meaning for all the parameters. Because the decrease of the slope with temperature is small, it is possible to divide the plot into small temperature intervals in each of which there is linear Arrhenius behavior. The A and ΔH values calculated for each interval will be assigned to the mean temperature of the interval and will be denoted by A_{LF_i} and ΔH_{LF_i}, so that we can write

$$\sigma T_i = A_{\mathrm{LF}_i} \exp(-\Delta H_{\mathrm{LF}_i}/kT) . \qquad (4)$$

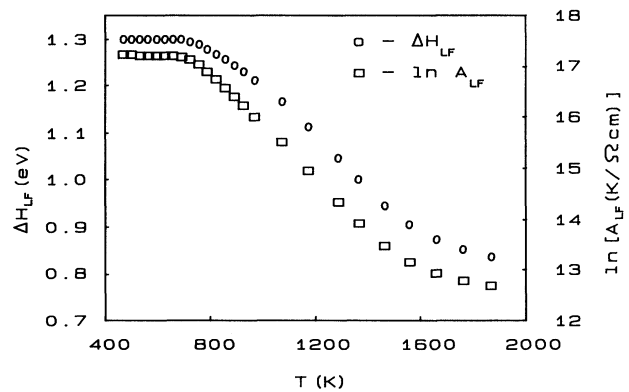The subscript indicates the interval in which the parameters were obtained. These values are plotted in Fig. 2.

FIG. 2. Values of ΔH_{LF} and A_{LF} obtained by the LF method vs absolute temperature.

The two plots have the same shape because, in the LF method, for a given temperature interval, ΔH_{LF_i} is obtained from the tangent to the experimental data and the preexponential term A_{LF_i} from the intersection with the conductivity axis. Hence A_{LF_i} has to follow the variation of the tangent over whole temperature range. This method can be applied only if changes in the slope are gradual.

By least-squares fitting the calculated ΔH_{LF_i}, it is possible to determine a temperature-dependence function of the activation enthalpy, $\Delta H(T)$. The best fit can be obtained using the function

$$\Delta H(T) = E_f + E_b \tanh[\beta(1/T - 1/T_f)] . \quad (5)$$

Here E_f, E_b, β, and T_f are adjustable temperature-independent parameters for which, in our case, the values are $E_f = 1.01$ eV, $E_b = 0.29$ eV, $\beta = 3278$ K, and $T_f = 1328$ K. The fit of Eq. (5) to the experimental values for ΔH_{LF_i} is shown in Fig. 3. It can be seen that $\Delta H(T)$ evolves from one steady state at low temperature ($\Delta H = 1.3$ eV for $T < 400\,°C$) asymptotically to another at high temperature with an activation enthalpy that is not well defined. Such behavior has been reported for many ceramic materials.[3-14]

From the activation enthalpy $\Delta H(T)$ [Eq. (5)], it is possible to deduce the variations of the entropy $\Delta S(T)$ and Gibbs energy $\Delta G(T)$ as[15-17]

$$\Delta S(T) = \Delta S_0 + \frac{\Delta H(T)}{T} + \int \frac{\Delta H(T)}{T^2} dT , \quad (6)$$

$$\Delta G(T) = \Delta H(T) - T \Delta S(T) , \quad (7)$$

with ΔS_0 an integration constant. Substituting Eq. (5) into Eqs. (6) and (7), we obtain

$$\Delta S(T) = (E_b/T)\tanh[\beta(1/T - 1/T_f)]$$
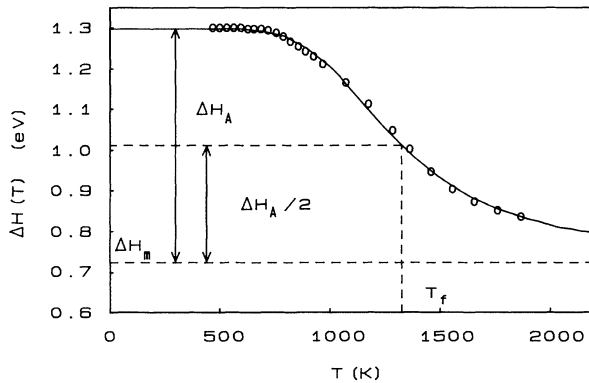$$- (E_b/\beta)\ln[\cosh\beta(1/T - 1/T_f)] + \Delta S_0 \quad (8)$$

and

$$\Delta G(T) = E_f + E_b(T/\beta)\ln[\cosh\beta(1/T - 1/T_f)] - T \Delta S_0 . \quad (9)$$

The integration constant ΔS_0 may be easily calculated from Eq. (8) by setting the temperature to T_f, so that ΔS_0 is given by $\Delta S(T_f)$.

In order to test whether the LF method gives a good representation of the problem, we can test the behavior of $\ln A_{LF_i}$ with respect to $\Delta S(T)$. Since[12,15,18]

$$A_{LF} = A_0 \exp\left[\frac{\Delta S(T)}{k}\right] , \quad (10)$$

by plotting $\ln A_{LF_i}$ versus $\Delta S'(T)/k$ [$\Delta S'(T) = \Delta S(T) - \Delta S_0$], we should have a straight line of slope 1. In Fig. 4 we show this plot for the 12 mol% Y_2O_3–ZrO_2 single crystals: The slope is 0.996, showing that our LF is a very good method for fitting the ionic conductivity in this compound.

IV. THEORETICAL MODEL FOR EQUALLY PROBABLE JUMPS

Let us now develop a microscopic model that allows us to interpret the results and to understand the physical meaning of the parameters in the empirical function Eq. (5).

The conductivity (σ) and the diffusion coefficient (D) of the vacancies are related by the Nernst-Einstein equation, which for weak electrical fields can be written as

$$\sigma = \frac{nq^2 D}{kT} , \quad (11)$$

where n is the carrier density and q is the charge.

We shall determine n and D for a cubic lattice by assuming that (i) the successive anionic jumps are not correlated, (ii) the diffusion takes place through nearest-neighbor (NN) oxygen vacancies, (iii) all the jumps have the same frequency, and (iv) the oxygen vacancies are randomly distributed.

With these assumptions, n (in our case, the number of

FIG. 3. ΔH_{LF} data and the empirical function $\Delta H(T)$ vs absolute temperature. The most important parameters of the best-fit function $\Delta H(T)$ are shown in the figure.
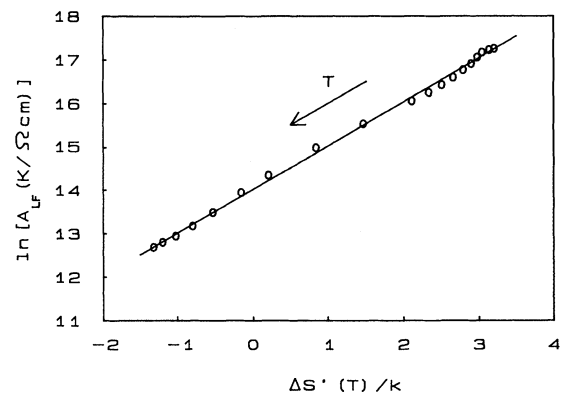

FIG. 4. Test of the LF method: $\ln A_{LF}$ vs $\Delta S'(T)/k$ [$\Delta S'(T) = \Delta S(T) - \Delta S_0$].

oxygen vacancies) can be written as

$$n = \frac{NN_v}{a^3 N'} , \tag{12}$$

where N is the number of anionic sites in the crystal, N_v is the volume fraction of vacancies, N' the number of unit cells, and a the lattice parameter. Since $N/N' = 8$, Eq. (12) can be rewritten as

$$n = 8N_v/a^3 . \tag{13}$$

The diffusion coefficient D is given by[19]

$$D = \frac{1}{2} \sum_{i=1}^{6} \Gamma_i \Delta x_i^2 = \Gamma a^2/4 , \tag{14}$$

where Γ_i is the frequency of jump i, Γ the average jump frequency, and Δx_i ($\Delta x_i = a/2$) the effective distance of a jump. To determine Γ at any temperature, we need to know the number of vacancies which participate in the conduction (N_c) and the average number per unit time able to overcome the potential barrier ΔG_m between two NN anionic sites ($\langle n_{\Delta G_m} \rangle$).

The probability that NN anionic positions are occupied by j oxygen vacancies ($0 \leq j \leq 6$) is

$$P_j = \binom{6}{j} N_v^j (1-N_v)^{6-j} . \tag{15}$$

With (N_{vf}) the fraction of the total vacancies free, the number of free vacancies will be nN_{vf}. If we now multiply this number by $\sum_{j=0}^{5} P_j$, we obtain the number of free vacancies (N_c),

$$N_c = nN_{vf} \sum_{j=0}^{5} P_j . \tag{16}$$

The term $j = 6$ is excluded because it represents a vacancy with six NN vacancies. As $\sum_{j=0}^{5} P_j = 1 - P_6$, Eq. (16) can be written as

$$N_c = nN_{vf}(1-N_v^6) . \tag{17}$$

The jump frequency (ω) is given by[19]

$$\omega = \nu_0 \exp\left[-\frac{\Delta G_m}{kT} \right] , \tag{18}$$

where ν_0 is the attempt frequency of the vacancy. If now we multiply N_c by ω and divide by n, we have

$$\langle n_{\Delta G_m} \rangle = N_{vf}(1-N_v^6)\nu_0\exp(-\Delta G_m/kT) . \tag{19}$$

Dividing Eq. (19) by the anionic vacancy coordination number[19] (6), we obtain

$$\Gamma = \frac{\nu_0 N_{vf}(1-N_v^6)}{6}\exp(-\Delta G_m/kT) , \tag{20}$$

and from Eqs. (11), (13), (14), and (20), we have

$$\sigma T = \frac{4\nu_0 e^2 N_{vf} N_v (1-N_v^6)}{3ka}\exp(-\Delta G_m/kT) , \tag{21}$$

where e is the electron charge.

In order to deduce the degree of dissociation[20] (N_{vf}),

we cannot use the mass action law because the structure and types of clusters are unknown in this sample. To determine the concentration of defects, a more general method is necessary such as the minimum-energy condition.[17,20] So the free energy of the dissociation process as a function of n_{vf} (free-vacancy number) has been obtained by using the Maxwell-Boltzmann statistic. Then, by imposing the minimum-energy condition with regard to n_{vf} and considering that n_{vf} is not negligible in relation to n, N_{vf} has been calculated (see Appendix A) as

$$N_{vf} = \frac{\exp[(-\Delta G_a/kT)-\ln Z_c]}{1+\exp[(-\Delta G_a/kT)-\ln Z_c]} , \tag{22}$$

where ΔG_a is the Gibbs free energy for vacancy association and Z_c the number of equivalent configurations of clusters. By substituting Eq. (22) into Eq. (21), we obtain

$$\sigma T = \frac{4\nu_0 e^2 N_v (1-N_v^6)}{3ka}$$
$$\times \frac{\exp\{-[(\Delta G_a + \Delta G_m)/kT]-\ln Z_c\}}{1+\exp[-(\Delta G_a/kT)-\ln Z_c]} . \tag{23}$$

Let us now determine the theoretical function $\Delta H(T)$. From Arrhenius's law, we can define $\Delta H(T)$ as

$$\Delta H(T) = -\frac{\partial \ln\sigma T}{\partial \alpha} , \tag{24}$$

with $\alpha = 1/kT$. By comparison with Eq. (21), we have

$$\Delta H(T) = -\frac{\partial \ln N_{vf}}{\partial \alpha} + \frac{\partial \alpha \, \Delta G_m}{\partial \alpha} . \tag{25}$$

If we assume that ΔH_a, ΔH_m, ΔS_a, and ΔS_m (enthalpy and entropy variations for the association and migration of the vacancies, respectively) are temperature independent, by means of Eq. (25) it is easy to calculate $\Delta H(T)$:

$$\Delta H(T) = \Delta H_m + \frac{\Delta H_a}{2}$$
$$+ \frac{\Delta H_a}{2}\tanh\left[\frac{\Delta H_a}{2kT} - \frac{\Delta S_a}{2k} + \frac{\ln Z_c}{2} \right] . \tag{26}$$

This equation has the same form as Eq. (5) obtained from the LF method.

We can also evaluate from Eq. (21) the preexponential factor of Arrhenius's law. The empirical form of this law for nonlinear behavior is

$$\sigma T = A(T)\exp\left[-\frac{\Delta H(T)}{kT} \right] , \tag{27}$$

with

$$A(T) = A_0\exp\left[\frac{\Delta S(T)}{k} \right] \tag{28}$$

and A_0 a constant dependent on the microscopic characteristics of the sample. By comparison of (21) and (27),

we obtain

$$\ln A\,(T)=\ln\frac{4e^2N_v(1-N_v^6)v_0}{3ka}$$

$$+\ln N_{vf}-\frac{\Delta G_m}{kT}+\frac{\Delta H(T)}{kT}\,.\tag{29}$$

Taking into account Eq. (25) and substituting Eq. (26) into Eq. (6), we have

$$\frac{\Delta S(T)}{k}=\frac{\alpha\,\Delta H_a}{2}\tanh\left[\frac{\alpha\,\Delta G_a}{2}+\frac{\ln Z_c}{2}\right]$$

$$-\ln\left[\cosh\left[\frac{\alpha\,\Delta G_a}{2}+\frac{\ln Z_c}{2}\right]\right]+\frac{\Delta S_0}{k}\,.\tag{30}$$

Substituting Eqs. (22) and (26) into (29), and taking into account Eq. (30), we can write

$$\ln A\,(T)=\ln\left[\frac{4v_0e^2N_v(1-N_v^6)}{3ka}\right]+\frac{\Delta S(T)}{k}\,,\tag{31}$$

if we assume that

$$\frac{\Delta S_0}{k}=\frac{\Delta S_a}{2k}+\frac{\Delta S_m}{k}-\frac{\ln Z_c}{2}-\ln 2\,.\tag{32}$$

By comparison of Eqs. (28) and (31), we obtain

$$A_0=\frac{4v_0e^2N_v(1-N_v^6)}{3ka}\,,\tag{33}$$

as a function of the microscopic parameters v_0 and a.

V. RESULTS AND DISCUSSION

This model allows us to determine the enthalpy for migration and association of the oxygen vacancies in clusters. Comparing Eqs. (5) and (26), we have

$$\Delta H_a=2E_b\,,\tag{34}$$

$$\Delta H_m=E_f-E_b\,,\tag{35}$$

$$\beta=\frac{\Delta H_a}{2k}\,,\tag{36}$$

$$\frac{\beta}{T_f}=\frac{\Delta S_a}{2k}-\frac{\ln Z_c}{2}\,.\tag{37}$$

From Eqs. (34)–(37), we can identify E_b with half of the enthalpy for clusters and E_f with the migration enthalpy for free vacancies plus half of the association enthalpy of the vacancies in clusters. Because E_b, E_f, and T_f are known, we can determine $\Delta H_a=0.57$ eV and $\Delta H_m=0.73$ eV ($\Delta H_a+\Delta H_m=1.30$ eV, which corresponds to the energy for the extrinsic associated state). There is a lack of published experimental data for these two magnitudes, because, although Arrhenius's law has a linear behavior at low temperatures (extrinsic associated range), this is not true[3] at high temperatures ($800\le T\le 1600\,^\circ$C). It is therefore not possible to determine ΔH_m with accuracy, and hence neither ΔH_a. However, these two enthalpies have been calculated by Bauerle and Hrizo[1] for samples of $[(ZrO_2)_{0.90}\text{-}(Y_2O_3)_{0.10}]$,

and by Badwal and Swain[8] for samples of $[(ZrO_2)_{0.88}\text{-}(Y_2O_3)_{0.12}]$ using two exponentials to fit the experimental resistivity between 400 and 1000 $^\circ$C. Bauerle and Hrizo obtained $\Delta H_a=0.49$ eV and $\Delta H_m=0.68$ eV, in agreement with our results (it is necessary to point out that the range of temperature they used is very narrow, and this is probably the origin of the small difference). Badwal and Swain, however, found $\Delta H_a=0.36$ eV and $\Delta H_m=0.91$ eV, in disagreement with our results. Using the same two-exponential method for our work ($200\,^\circ$C$\le T\le 1600\,^\circ$C), we obtain $\Delta H_a=0.61$ eV and $\Delta H_m=0.69$ eV, similar to the values obtained with our LF method and in agreement with the values of Bauerle and Hrizo.

With respect to the published theoretical values[22-24] for ΔH_m, when ZrO_2 is doped with Y_2O_3 they range from 0.8 eV (Ref. 23) to 0.9 eV,[24] being significantly larger than the one obtained with our fit. With respect to ΔH_a, the theoretical value obtained by Bingham, Tasker, and Cormack,[24] 0.6 eV for clusters of type $[V_0Y'_{Z_r}]_{NN}$, and by Butler, Catlow, and Fender,[22] 0.63 eV for clusters of type $[Y'_{Z_r}V_0Y'_{Z_r}]^x$, are both in agreement with the one obtained from our model.

An apparently surprising result of the theoretical model is that it seems to show that ionic defects behave as fermions, because the free-energy dependence of N_{vf} [Eq. (22)] is similar to a Fermi-Dirac distribution function. However, this equation is a free-energy function, but it is not function of the energy of the particle state, and therefore it is not a distribution function. There is a classical system with a similar Fermi-Dirac behavior: the two-state system of N independent particles.[21] If ε_1 and ε_2 are the energies of the two states, the distribution function is given by[25]

$$n_i=-\frac{1}{\gamma}\frac{\partial\ln Z}{\partial\varepsilon_i}\,,\tag{38}$$

with $Z=[\exp(-\gamma\varepsilon_1)+\exp(-\gamma\varepsilon_2)]^N$ the partition function for this system and $\gamma=1/kT$. As $\Delta\varepsilon=\varepsilon_2-\varepsilon_1$, we obtain

$$n_2/N=\frac{\exp(-\gamma\,\Delta\varepsilon)}{1+\exp(-\gamma\,\Delta\varepsilon)}\,,\tag{39}$$

which is similar to the Fermi-Dirac distribution function. The vacancy-dissociation process can be considered as a two-state system in this model if ε_1 and ε_2 are taken as the energies of the dissociate and associate states of the vacancies, respectively.

On the other hand, the same expression for N_{vf} [Eq. (22)] is obtained with an alternate classical statistical procedure (classic approximation). Let us consider the anionic lattice in the crystal with N anionic sites and n vacancies. The partition function can be factorized as[20]

$$Z=Z_{\text{conf}}Z_v\,,\tag{40}$$

where Z_{conf} is the configurational term and Z_v is the vibrational factor. If n_{vf} of this vacancy has an energy ε_{d1} and $n-n_{vf}$ an energy ε_{d2} ($n\ge n_{vf}$), Z_{conf} is given by

$$Z_{\text{conf}} = \frac{N!}{(n - n_{vf})! n_{vf}! (N - n)!} Z_c^{n - n_{vf}} Z_f^{n_{vf}} , \qquad (41)$$

where Z_c and Z_f are the number of energy-equivalent configurations that one vacancy has due to the presence of dopant cations in the cationic lattice.

In the high-temperature approximation, Z_v can be written as[20]

$$Z_v = \exp \left[-\frac{\phi'}{kT} \right] \prod_i \frac{kT}{h v_i'} , \qquad (42)$$

where ϕ' is the cohesive energy for the defective crystal and v_i' the modified normal-mode frequencies. If the interactions among defects are ignored, then

$$\phi' = \phi + n_{vf} \varepsilon_{d1} + (n - n_{vf}) \varepsilon_{d2} , \qquad (43)$$

and if the Einstein approximation is assumed and it is assumed that the vacancies modify the vibrational frequency of only a few neighboring atoms, e.g., the p_1 and p_2 nearest neighbors for the vacancies in ε_{d1} and ε_{d2}, respectively, then

$$Z_v(n, n_{vf}) = \frac{(kT)^{3N} \exp(-\phi'/kT)}{(h v')^{n_{vf} p_1} (h v'')^{(n - n_{vf}) p_2} (v)^{3N - n_{vf} p_1 - (n - n_{vf}) p_2}}$$

$$= Z_v(0,0) [\exp(-\varepsilon_{d1}/kT)(v/v')^{p_1}]^{n_{vf}} [\exp(-\varepsilon_{d2}/kT)(v/v'')^{p_2}]^{n - n_{vf}} , \qquad (44)$$

with $Z_v(0,0)$ the partition function in the absence of vacancies.

The thermodynamic potentials for the defective crystal can be obtained from the partition function[20] and can be written as

$$G_v(n, n_{vf}) = G_0 + n_{vf} \varepsilon_{d1} + (n - n_{vf}) \varepsilon_{d2}$$

$$- n_{vf} kT \ln[(v/v')^{p_1}]$$

$$- (n - n_{vf}) kT \ln[(v/v'')^{p_2}] , \qquad (45a)$$

$$S_v(n, n_{vf}) = S_0 + n_{vf} kT \ln[(v/v')^{p_1}]$$

$$- (n - n_{vf}) kT \ln[(v/v'')^{p_2}] , \qquad (45b)$$

$$H_v(n, n_{vf}) = H_0 + n_{vf} \varepsilon_{d1} + (n - n_{vf}) \varepsilon_{d2} , \qquad (45c)$$

G_0, H_0, and S_0 being the thermodynamic potentials of the perfect crystal.

The full thermodynamic potentials are obtained by adding the vibrational part to the configurational potential derived from Eq. (41),

$$G_{\text{conf}}(n, n_{vf}) = -kT \ln \left[\frac{N!}{(N - n)! n!} \right]$$

$$- kT \ln \left[\frac{n!}{(n - n_{vf})! n_{vf}!} Z_c^{n - n_{vf}} \right]$$

$$- kT \ln[Z_f^{n_{vf}}] . \qquad (46)$$

Assuming that n is independent of the temperature, the total free energy can be written as

$$G_T(n_{vf}) = G_{0_T} + n_{vf}(\Delta H_a - T \Delta S_a) - T \Delta S_{\text{conf}}$$

$$= G_{0_T} + n_{vf} \Delta G_a - \Delta S_{\text{conf}} , \qquad (47)$$

where

$$G_{0_T} = G_0 - kT \ln \left[\frac{N!}{(N - n)! n!} \right] , \qquad (48a)$$

$$\Delta H_a = \varepsilon_{d1} - \varepsilon_{d2} , \qquad (48b)$$

$$\Delta S_a = k \ln[(v/v')^{p_1}] - k \ln[(v/v'')^{p_2}] + k \ln Z_f , \qquad (48c)$$

$$\Delta S_{\text{conf}} = k \ln \left[\frac{n!}{(n - n_{vf})! n_{vf}!} Z_c^{n - n_{vf}} \right] . \qquad (48d)$$

If we consider $\Delta G(T) = G_T(n_{vf}) - G_{0_T}$, we obtain our Eq. (A2), and imposing the minimum-energy condition

$$\frac{\partial G_T(n_{vf})}{\partial n_{vf}} = \frac{\partial \Delta G(T)}{\partial n_{vf}} = 0 ,$$

we obtain the Eq. (A4). Therefore Eq. (22) represents a classical statistical behavior.

With the proposed model, it is possible to determine N_{vf}. Thus, from Eqs. (36) and (37), we have

$$-\frac{\Delta G_a}{kT} - \ln Z_c = 2\beta \left[\frac{1}{T_f} - \frac{1}{T} \right] , \qquad (49)$$

so that Eq. (22) can be rewritten as

$$N_{vf} = \frac{\exp[2\beta(1/T_f - 1/T)]}{1 + \exp[2\beta(1/T_f - 1/T)]} . \qquad (50)$$

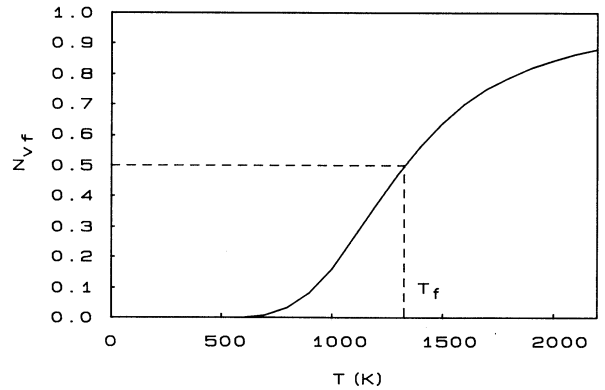Figure 5 shows a plot of N_{vf} versus T for temperatures

FIG. 5. Degree of dissociation of vacancies (N_{vf}) vs absolute temperature.

ranging from 0 to 2273 K. One can see that the extrinsic dissociation state goes up to approximately 673 K, where all the vacancies form clusters ($N_{vf} \simeq 0$). The parameter T_f is defined as the temperature at which half the vacancies are free ($N_{vf} = 0.5$). At a temperature of 1873 K (maximum in this work), $N_{vf} = 0.81$, so that the extrinsic dissociated stage has not been reached. This theoretical result is in agreement with the non-Arrhenius behavior found experimentally in these systems.[3]

To make an estimation of $\Delta S(T)$ and $\Delta G(T)$, we need to know ΔS_0 [Eq. (6)]. This can be done by using the boundary condition[16] $\Delta S(T = \infty) = 0$, which together with Eq. (8) yields $\Delta S_0/k = 1.810$. To see if this value is physically acceptable, we shall calculate the attempt frequency ν_0 from A' given by Arrhenius's law:

$$A' = A_0 \exp(\Delta S_0/k) , \qquad (51)$$

A' being the ordinate at the origin in Fig. 4. From Eqs. (33) and (51), we obtain $\nu_0 = 7.83 \times 10^{13}$ Hz, about 4 times larger than the maximum frequency for the lattice vibrational modes in zirconia, 2.07×10^{13} Hz (ν_0^{si} in Fig. 6), obtained from hyper-Raman-scattering experiments by Shin and Ishigame.[26] This discrepancy may be because our model considered only jumps between nearest neighbors [we shall denote them by first neighbors (1N)]. If we consider jumps between next-nearest neighbors (NNN) too [second neighbors (2N)] or between NN, NNN, and second-next-nearest neighbor [third neighbors (3N)], the preexponential factors will be (Appendix B)

$$A_0^{2N} = \frac{4e^2 N_v \nu_0}{ka} \qquad (52)$$

and

$$A_0^{3N} = \frac{8e^2 N_v \nu_0}{ka} , \qquad (53)$$

respectively. In Fig. 6 we represent $\Delta S/k$ for $T = \infty$ versus the attempt frequency running from 10^{13} to 10^{14} Hz. The entropy variation was calculated from Eq. (51)
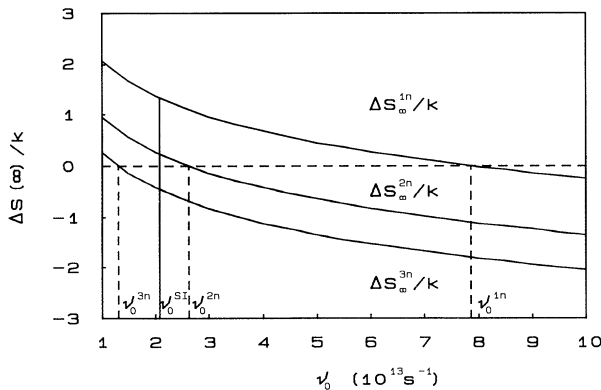
using Eqs. (33), (52), and (53), giving, in obvious notation, ΔS_∞^{1N}, ΔS_∞^{2N}, and ΔS_∞^{3N}, respectively. In Fig. 6 we also show the frequencies $\nu_0^{1N} = 7.83 \times 10^{13}$ Hz, $\nu_0^{2N} = 2.62 \times 10^{13}$ Hz, and $\nu_0^{3N} = 1.31 \times 10^{13}$ Hz, which satisfied the condition $\Delta S(\infty) = 0$ for each approximation. The solid line is ν_0^{si}. One observes that ν_0^{3N} lies in the range of the lattice vibrational modes in zirconia[26] and is in agreement with the accepted value of the attempt frequency.[1,12] We shall therefore regard ν_0^{3N} (contribution of jumps 1N, 2N, and 3N) as the attempt frequency for the oxygen vacancies ($\nu_0 = 1.31 \times 10^{13}$ Hz).

We can now represent the behavior of $\Delta S(T)$ and $\Delta G(T)$ in the ionic conductivity process for our samples (Fig. 7). This behavior is similar to that found by Wang in Na β''-alumina,[16] who suggested a steady state (extrinsic associated domain) at low temperatures and asymptotic behavior at high temperatures, as in our model.

VI. CONCLUSION

The ionic conductivity of a ZrO_2–12 mol % Y_2O_3 single crystal was described with an empirical function in the temperature range from 200 to 1600 °C. This function was determined by using a local-fit method to fit the experimental data to the Arrhenius law. In order to understand the physical meaning of the fitted parameters, a microscopic two-state theoretical model was developed, from which the enthalpies of migration (0.73 eV) and association in clusters (0.57 eV) of the vacancies were calculated. Moreover, we can determine the fraction of free vacancies to a given temperature, which shows a functional form similar to a Fermi-Dirac distribution function, although it was deduced using the classical approximation. On the other hand, the attempt frequency value of 1.31×10^{13} Hz for oxygen-vacancy hopping was determined as well. Finally, the behavior of the free energy and entropy of the conduction process was analyzed. It was found that the temperature-dependence behavior is similar to what was pointed out by Wang in Na β''-alumina samples.[16] Therefore the proposed microscopic model not only allow us to represent the ionic conductivity-temperature dependence, but also to know some important physical parameters such as the enthalpies of the vacancies in each state (free or bound) and to

FIG. 6. Values of $\Delta S(T)$ for $T = \infty$ obtained with the first (ΔS_∞^{1N}), second (ΔS_∞^{2N}), and third (ΔS_∞^{3N}) anionic neighbors with the attempt frequency running from 10^{13} to 10^{14} Hz. ν_0^{si} is the maximum frequency for the lattice vibrational modes in zirconia from Ref. 26.
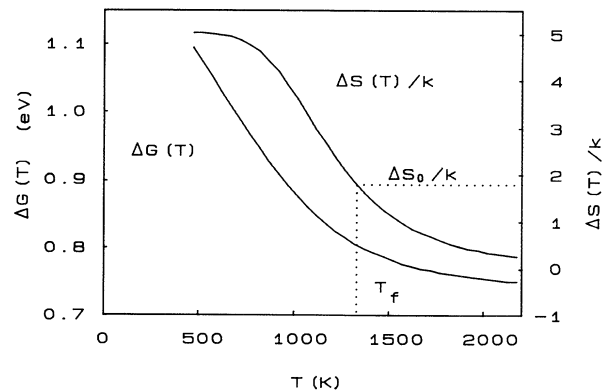

FIG. 7. Temperature dependence of the functions $\Delta S(T)$ and $\Delta G(T)$ obtained from the function $\Delta H(T)$, with the condition $\Delta S(\infty) = 0$.

understand in a very intuitive way the dynamic of ionic defects in these crystals.

ACKNOWLEDGMENT

APPENDIX A

In order to determine N_{vf}, we shall use the Maxwell-Boltzmann statistic. Let us assume that there are n vacancies, of which n_{vf} are free (not forming clusters). If ΔG_a is the energy necessary to set a vacancy free,

$$\Delta G_a = \Delta H_a - T\,\Delta S_a \ , \tag{A1}$$

the energy to set n_{vf} free will be

$$\Delta G(T) = n_{vf}\Delta G_a - T\,\Delta S_{\text{conf}} \ , \tag{A2}$$

where ΔS_{conf} (configurational entropy) can be written as

$$\Delta S_{\text{conf}} = k\,\ln[\,(^{n}_{n_{vf}})Z_c^{(n-n_{vf})}\,] \ . \tag{A3}$$

Imposing the minimum-energy condition with regard to n_{vf} with Stirling's approximation[21] and considering that n_{vf} is not negligible in relation to n, we obtain

$$\Delta G_a = -kT\ln\left[\frac{n_{vf}}{n-n_{vf}}\right] - kT\ln Z_c \tag{A4}$$

or, as a function of $N_{vf} = n_{vf}/n$ (degree of dissociation[20]),

$$N_{vf} = \frac{\exp(-\Delta G_a/kT - \ln Z_c)}{1 + \exp(-\Delta G_a/kT - \ln Z_c)} \ . \tag{A5}$$

APPENDIX B

In the model developed in this article, we considered jumps between nearest neighbors (1N). In this appendix we shall evaluate the contribution of next-nearest neighbors (2N) and of the second-next-nearest neighbors (3N).

In the fluorite structure, we have 6 (1N) positions, 12 (2N), and 8 (3N). First, consider jumps between 1N and 2N. In this case, Eq. (14) (see Sec. IV) is modified to

$$D = \frac{a^2}{4}\Gamma_{1N} + a^2\Gamma_{2N} \ , \tag{B1}$$

where Γ_{1N} and Γ_{2N} are the frequencies for jumps 1N and 2N, respectively. These frequencies can be calculated as in Eq. (20) (Sec. IV):

$$\Gamma_{1N} = \frac{v_0(1-N_v^6)N_{vf}}{6}\exp\left[-\frac{\Delta G_m^{1N}}{kT}\right] \ , \tag{B2}$$

$$\Gamma_{2N} = \frac{v_0(1-N_v^8)N_{vf}}{12}\exp\left[-\frac{\Delta G_m^{2N}}{kT}\right] \ , \tag{B3}$$

with ΔG_m^{1N} and ΔG_m^{2N} the potential barriers for jumps 1N and 2N. If we keep all the hypotheses of the model except the second (see Sec. IV) and we assume that $\Delta G_m^{1N} \simeq \Delta G_m^{2N} \simeq \Delta G_m$, then D can be written as

$$D = v_0 a^2 N_{vf}\exp\left[-\frac{\Delta G_m}{kT}\right]\left[\frac{1-N_v^6}{24} + \frac{1-N_v^8}{12}\right] \ . \tag{B4}$$

If C_0 is the mole fraction of Y$_2$O$_3$ and because a V_0 is created from each pair of Y^{3+}, we can write

$$N_v = \frac{C_0}{2(1+C_0)} \ . \tag{B5}$$

In our case, $C_0 = 0.12$, and so $N_v = 0.053$. Then, if we put $1-N_v^6 \simeq 1-N_v^8 \simeq 1$ in Eq. (B4) and substitute it into Eq. (11) (Sec. IV),

$$\sigma T = \frac{4e^2 v_0 N_v}{ak}N_{vf}\exp\left[-\frac{\Delta G_m}{kT}\right] \ , \tag{B6}$$

from which the preexponential factor A_0^{2N} can be written as

$$A_0^{2N} = \frac{4e^2 v_0 N_v}{ak} \ . \tag{B7}$$

If now we consider the three types of jump (1N, 2N, and 3N), we should add the contribution of jump 3N to Eq. (B1). For that, we have to consider only four of the eight 3N positions, because the other four involve overcoming a cation. Hence

$$D = \frac{a^2}{4}\Gamma_{1N} + a^2\Gamma_{2N} + \frac{a^2}{2}\Gamma_{3N} \ , \tag{B8}$$

Γ_{3N} being given by

$$\Gamma_{3N} = \frac{v_0(1-N_v^4)N_{vf}}{4}\exp\left[-\frac{\Delta G_m^{3N}}{kT}\right] \ . \tag{B9}$$

With the same simplification as before,

$$\sigma T = \frac{8e^2 v_0 N_v}{ka}N_{vf}\exp\left[-\frac{\Delta G_m}{kT}\right] \tag{B10}$$

and

$$A_0^{3N} = \frac{8e^2 v_0 N_v}{ka} \ . \tag{B11}$$

[1]J. E. Bauerle and J. Hrizo, J. Phys. Chem. Solids **30**, 565 (1969).

[2]E. Schouler, G. Giroud, and M. Kleitz, J. Chem. Phys. (Paris) **70**, 1309 (1973).

[3]Y. Suzuki, T. Takahashi, and N. Nagae, Solid State Ionics **3-4**, 483 (1981).

[4]P. Abelard and J. F. Baumard, Phys. Rev. B **26**, 1005 (1982).

[5]J. F. Baumard and P. Abelard, in *Science and Technology of Zirconia II*, edited by N. Claussen, M. Rühle, and A. H. Heuer, *Advances in Ceramics*, Vol. 12 (American Ceramic Society, Columbus, OH, 1984).

[6]M. Kleitz, H. Bernard, E. Fernandez, and E. Schouler, in *Science and Technology of Zirconia*, edited by A. H. Heuer and

L. W. Hobbs, *Advances in Ceramics,* Vol. 3 (American Ceramic Society, Columbus, OH, 1981).

[7]S. P. S. Badwal, J. Mater. Sci. **19**, 1767 (1984).

[8]S. P. S. Badwal and M. V. Swain, J. Mater. Sci. Lett. **4**, 487 (1985).

[9]G. Chiodelli, A. Magistris, M. Scagliotti, and F. Parmigiani, J. Mater. Sci. **23**, 1159 (1988).

[10]R. Z. D. Fernandez, A. Hammou, and A. Hammouche, Solid State Ionics **37**, 31 (1989).

[11]J. A. Kilner and R. J. Brook, Solid State Ionics **6**, 237 (1982).

[12]A. S. Nowick, in *Diffusion in Crystalline Solids,* Materials Science Series, edited by G. E. Murch and A. S. Nowick (Academic, London, 1984).

[13]J. B. Bates and J. C. Wang, Solid State Ionics **28-30**, 115 (1988).

[14]Y. Suzuki and K. Sugiyama, J. Ceram. Soc. Jpn. Int. Ed. **95**, 480 (1987).

[15]I. Cachadiña, J. D. Solier, and F. L. Cumbrera, Bol. Soc. Esp. Ceram. Vidrio **30**, 493 (1991).

[16]J. C. Wang, Phys. Rev. B **26**, 5911 (1982).

[17]R. A. Swalin, *Thermodynamics of Solids,* 2nd ed. (Wiley, New York, 1972).

[18]J. A. Kilner and B. C. H. Steele, in *Nonstoichiometric Oxides,* Materials Science Series, edited by O. T. Sørensen (Academic, New York, 1981).

[19]J. Philibert, *Atom Movements. Diffusion and Mass Transport in Solids,* Monographies de Physique (Les éditions de Physique, Les Ulis, France, 1991).

[20]F. Agullo-Lopez, C. R. A. Catlow, and P. P. Townsend, *Point Defects in Materials* (Academic, London, 1988).

[21]C. Kittel, *Thermal Physics* (Wiley, New York, 1973).

[22]V. Butler, C. R. A. Catlow, and B. E. F. Fender, Solid State Ionics **5**, 1 (1981).

[23]W. C. Mackrodt and Woodrow, J. Am. Ceram. Soc. **69** (3), 277 (1986).

[24]D. Bingham, P. W. Tasker, and A. N. Cormack, Philos. Mag. A **60**, 1 (1989).

[25]F. Reif, *Fundamentals of Statistical and Thermal Physics* (McGraw-Hill, New York, 1965).

[26]S. Shin and M. Ishigame, Phys. Rev. B **34**, 233 (1986).